Paper

Bio-mimicry Sound Source Localization with Gimbal Diaphragm

Nobutaka Ono* Member
Akihito Saito* Non-member
Shigeru Ando* Member

The parasitoid fly *Ormia Ochracea* shows a remarkable ability to detect the direction of an incident sound even though its ears are in very close to each other, where the interaural differences in intensity and time are extremely small. In this paper, with mimicking the unique auditory organ of the fly, we propose a sound source localization mechanisms with *a gimbal diaphragm* which realizes a simple and optimal transduction mechanism for a very small pressure gradient caused by the sound field. We made a model sensor using a thin metal plate and confirmed that it localizes the direction of the sound source by experiments.

Keywords: fly, bio-mimicry sensor, micro sensor, sound source localization, gimbal

1. Introduction

Sound source localization is one of the most important function of auditory systems. Many animals with two ears use interaural intensity difference(IID) and time difference(ITD) as primary cues [1] [2]. Generally, ears in animals are separated with a significant distance in order to detect IID and ITD easily. This is also true for man-made systems using a microphone array. This is the reason why minituarization of the sound source localization system is very difficult.

However, the parasitoid fly *Ormia ochracea* shows a remarkable ability to detect the direction of an incident sound. Even though its acoustic sensory organs are in very close (about 500[μm]) to each other, it localizes the song of the cricket whose wavelength is about 75[mm], where IID and ITD can be extremely small [3]~[6]. The directional hearing in such a surprising size is achieved by its unique structure of the auditory organ.

The goal of our research is a realization of a micro sound source localization sensor with mimicking the excellent ears of the fly. In our previous study [7], we summarized its key structures to 1) center-supported diaphragm, and 2) enhancement mechanism to reversed-phase vibration. The problem is how to realize them as a sensor.

In this paper, as an answer to it, we propose a novel transduction mechanism, *gimbal diaphragm*, which enables to detect both the sound pressure and the tiny sound gradient independently by three vibration modes of a thin circular plate. We show an algorithm to localize the sound source combining the three vibration signals of the diaphragm. We show our fabricated sensor and confirm that 1) it detects a very small sound gradient, 2) it localizes the direction of the sound source as the theory.

* Dept. Information Physics and Computing, University of Tokyo 7-3-1 Hongo, Bunkyo-ku, Tokyo, 113-8656

2. Modeling Auditory Organ of Ormia Ochracea

2.1 Mathematical Preparation Here, we summarize properties of a sound field on a micro diaphragm. Let $P(x, y, z; t)$ be a sound pressure on the diaphragm, which is in the x-y plane and whose center is at the origin. Assume that the dimension of the diaphragm is much smaller than a wavelength. Then, by the Taylor expansion, $P(x, y, z; t)$ is approximately written as

$$P(x, y, z; t) \simeq P(t) + P_x(t) \cdot x + P_y(t) \cdot y, \cdots (1)$$

where $P(t)$ represents $P(0, 0, 0; t)$ and suffixes x and y represent spatial derivatives. Eq.(1) shows that the sound field on the micro diaphragm is decomposed into 1) a spatially uniform force, 2) a moment about y axis, 3) a moment about x axis. The relationship between sound field gradient and sound source direction is given by the following equations.

$$P_x(t) = -\frac{\sin\phi\cos\theta}{c}\dot{P}(t), \cdots (2)$$

$$P_y(t) = -\frac{\sin\phi\sin\theta}{c}\dot{P}(t), \cdots (3)$$

where θ and ϕ are defined as Fig.1 and c represents the sound velocity. It is necessary to detect all terms for sound source localization [9].

2.2 Interpretation of the fly's ear structure In recent years, the anatomy of the auditory organ of the fly and its vibration modes have been the subject of many studies [3]~[5]. The remarkable features of it(Fig.3) are summarized as: 1) The fly's left and right ears are not separated but contained within a common air-filled chamber [4]. 2) The center of the membrane doesn't vibrate and works as the pivot of vibrations [5]. 3) The left and right parts of the membrane are connected by a mechanical coupling [5].

As discussed in [7], we interpret the features as follows: 1) The diaphragm with supported at the center pivot is

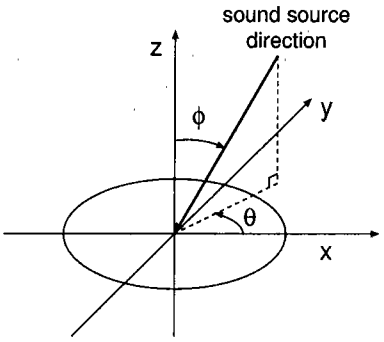

Fig. 1. The definition of the coordinate system.

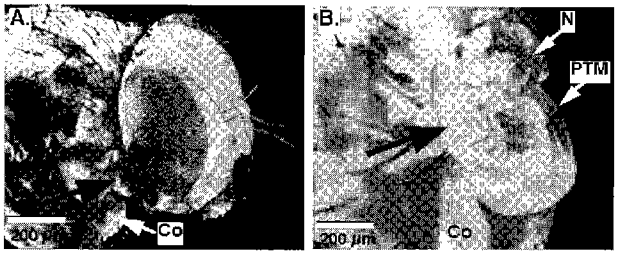

Fig. 2. External anatomy of *Ormia ochracea* before (A) and after (B) surgical removal of the head [8]: The tips of arrows in the figure indicate the auditory organ, which is located behind the head.

an optimal mechanism to detect a small sound gradient because the sound gradient (the moment) transmits the diaphragm with no reaction force (Fig.4), 2) The mechanical coupling works as an enhancement mechanism for the vibration caused by the moment because it generates reaction only when the spatially uniform force works.

3. Sensor Design

3.1 Gimbal Diaphragm In order to realize a micro sensor which localizes a sound source in any direction, we introduce the two mechanisms discussed above to a sensor. The point is how to form a center-supported diaphragm which easily inclines to any directions.

In this paper, we propose a *gimbal diaphragm* shown in Fig.5 , which consists of 1) inner beams, 2) outer beams, 3) ring, 4) center region, and 5) diaphragm region. When the center region is fixed, this diaphragm has three vibration modes driven by three terms in eq.(1), independently. When a moment works, torsions of narrow inner and outer beams permit the diaphragm region to incline to any direction, and the both of ends of the diaphragm vibrates the opposite direction (reversed-phase vibration modes). While, a sound pressure works, the ring is deformed and all ends of the diaphragm vibrates the same direction (in-phase vibration). Then, the sensitivity for in-phase driving force can be controlled by designing the radius and the width of the ring. Therefore, the gimbal diaphragm realizes 1)center-supported diaphragm, 2)sensitivity control mechanism to in-phase driving force, by the simple and planar structure.

3.2 Vibration Model of Gimbal Diaphragm When the direction of sound source is (ϕ, θ), the resultant force and moments acting the diaphragm are given by

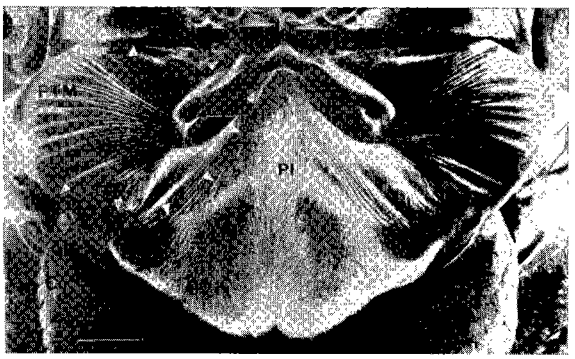

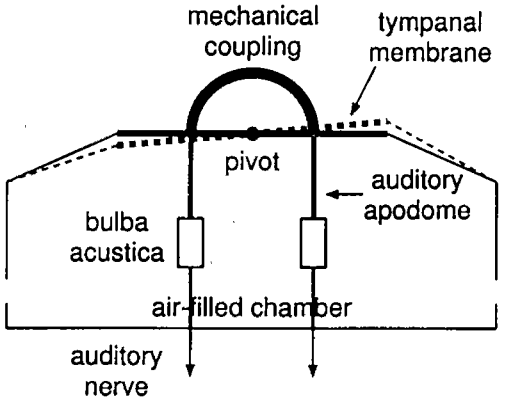

Fig. 3. Frontal views of the ears with the head removed [4](upper) and its diagram(lower): The vibrations in the left and right parts of the tympanum are transferred to a pair of auditory sensory organs, the bulbae acusticae through a stiff cuticular rod, auditory apodeme.

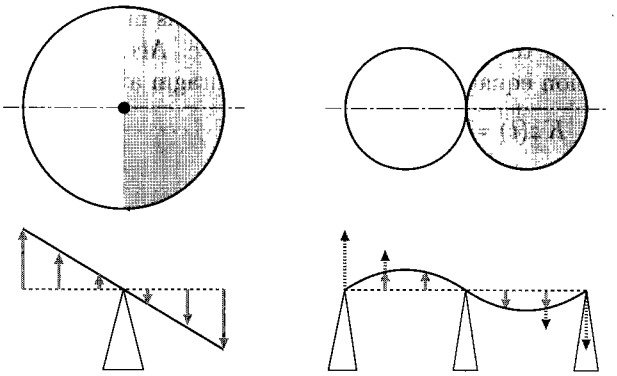

Fig. 4. The comparison with modes driven by the sound pressure gradient: While any reaction force doesn't work a center-supported diaphragm (left), the fixed ends of diaphragms in conventional microphones generate the reaction, and the effective force driven vibrations degrades (right).

$$F(t) = \int_0^a \int_0^{2\pi} P(t) r dr d\psi = \pi a^2 P(t), \quad \cdots\cdots (4)$$

$$N_x(t) = \int_0^a \int_0^{2\pi} \frac{\sin\phi\cos\theta}{c} \dot{P}(t) \cdot (r\cos\psi)^2 r dr d\psi = \frac{\pi a^4}{4c} \sin\phi\cos\theta \dot{P}(t), \quad \cdots\cdots (5)$$

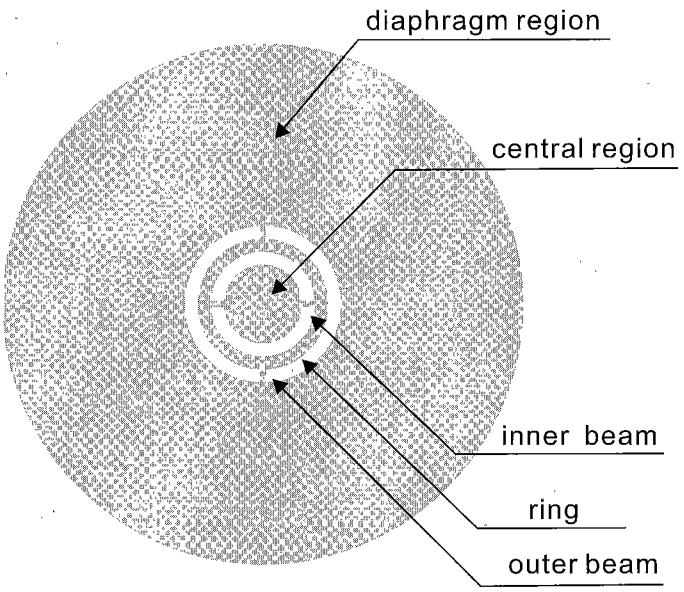

Fig. 5. A design of the gimbal diaphragm.

$$N_y(t) = \int_0^a \int_0^{2\pi} \frac{\sin\phi \sin\theta}{c} \dot{P}(t) \cdot (r\cos\psi)^2 r dr d\psi$$
$$= \frac{\pi a^4}{4c} \sin\phi \sin\theta \dot{P}(t), \cdots\cdots\cdots\cdots\cdots (6)$$

where a is the radius of the diaphragm. In the in-phase vibration mode, the flexural-rigidity of the ring generates a dominant reaction since inner and outer beams cannot expand. While in the reversed-phase vibration modes, the moment of inertia determines its mechanical impedance when inner and outer beams are sufficiently narrow to neglect their reaction force. Accordingly, the motion equations of a gimbal diaphragm are written as

$$Kz(t) = \pi a^2 P(t), \cdots\cdots\cdots\cdots\cdots\cdots\cdots\cdots (7)$$
$$I\ddot{\alpha}_x(t) = \frac{\pi a^4}{4c} \sin\phi\cos\theta \dot{P}(t), \cdots\cdots\cdots\cdots\cdots (8)$$
$$I\ddot{\alpha}_y(t) = \frac{\pi a^4}{4c} \sin\phi\sin\theta \dot{P}(t), \cdots\cdots\cdots\cdots\cdots (9)$$

where K is the stiffness of the ring, I is the moment of inertia, z, α_x, and α_y are the displacement and the angles of the diaphragm, respectively.

3.3 Theory of Sound Source Localization Let $< f(t), g(t) >$ be a correlation between $f(t)$ and $g(t)$ in a short time, Γ as

$$< f(t), g(t) > = \int_\Gamma f(t)g(t)dt. \cdots\cdots\cdots\cdots\cdots (10)$$

Eq.(7), eq.(8), eq.(9) indicate that $\dot{\alpha}_x(t)$, $\dot{\alpha}_y(t)$ code the information of the sound source directions and $z(t)$ works as a carrier signal. The correlation between each signal and $z(t)$ is written as

$$< z(t), z(t) > = \frac{\pi^2 a^4}{K^2} < P(t), P(t) >, \cdots\cdots\cdots (11)$$
$$< z(t), \dot{\alpha}_x(t) > = \frac{\pi^2 a^6}{4KI} \frac{\sin\phi\cos\theta}{c} < P(t), P(t) >, (12)$$
$$< z(t), \dot{\alpha}_y(t) > = \frac{\pi^2 a^6}{4KI} \frac{\sin\phi\sin\theta}{c} < P(t), P(t) > . (13)$$

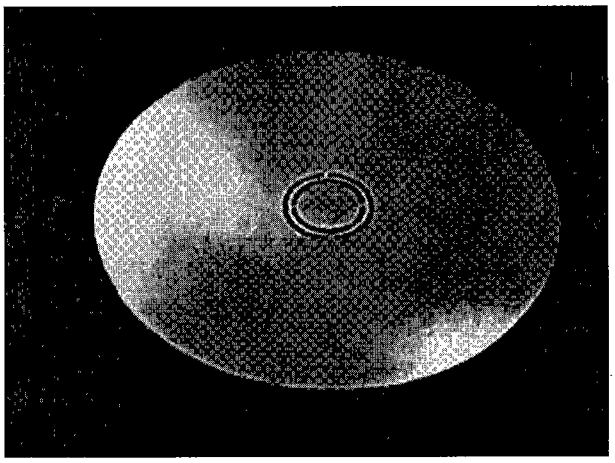

Fig. 6. A picture of fabricated gimbal diaphragm.

Table 1. Size parameters of our fabricated gimbal diaphragm.

parameters	values
radius of diaphragm	10.8[mm]
radius of center part	1.5[mm]
radius of ring	1.8[mm]
length of beam	0.2[mm]
width of beam	0.2[mm]
width of ring	0.2[mm]

By eliminating $< P(t), P(t) >$ and normalizing, we obtain

$$S_x = \frac{1}{C} \frac{< z(t), \dot{\alpha}_x(t) >}{< z(t), z(t) >} = \sin\phi\cos\theta, \cdots\cdots (14)$$
$$S_y = \frac{1}{C} \frac{< z(t), \dot{\alpha}_y(t) >}{< z(t), z(t) >} = \sin\phi\sin\theta, \cdots\cdots (15)$$

where

$$C = \frac{Ka^2}{4cI}. \cdots\cdots\cdots\cdots\cdots\cdots\cdots\cdots (16)$$

Therefore, the sound source directions are estimated by

$$\theta = \arctan\frac{S_y}{S_x}, \cdots\cdots\cdots\cdots\cdots\cdots\cdots (17)$$
$$\phi = \arcsin\sqrt{S_x^2 + S_y^2}. \cdots\cdots\cdots\cdots\cdots\cdots (18)$$

3.4 Fabrication Fig.6 shows a gimbal diaphragm, which we fabricated by etching 30[μm]-thickness phosphor bronze foil. Size parameters are shown in Table 1 . We designed the width of the inner and outer beams narrow enough to neglect reaction force. The width of the ring is also an important parameter to control the sensitivity in the in-phase mode. In this fabrication, we determined it experimentally. The derivation of the quantitative design rule is a future work. Its center region is fixed the pole as shown in Fig.7 . In order to prevent the incident sound pressure from leaking to the back, we surrounded the sensor by an aluminum pipe with a small gap.

4. Experiments

4.1 Conditions In order to confirm that 1) the

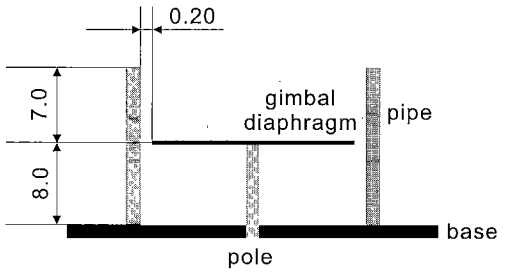

Fig. 7. The structure of our sensor.

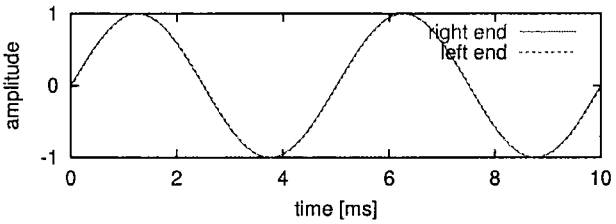

Fig. 8. The sound pressure on the right and the left end of the diaphragm (about 20[mm] distance) when 200[Hz] sinusoid arrives from $\phi = \pi/12$ direction. The phase difference is less than 1/300.

gimbal diaphragm detects a tiny acoustic gradient, 2) the sound source can be localized as discussed in Sec.(3.3), we examined the vibration of our fabricated diaphragm. The sound is given from nine directions: $\{(\phi, \theta) \mid \phi = \pi/12,\ \theta = n\pi/4\ (n = 1\sim 8)\}$ and $\phi = 0$. As a sound source signal, we chose 200Hz sinusoid so that the ratio of the diaphragm dimension to the wavelength of the incident sound is the same as the case of the parasitoid fly. Note that the phase difference of the sound pressure between both end of the diaphragm are very small (less than 1/300) in this condition as shown in Fig.8 .

4.2 Methods Fig.9 shows a schematic diagram of our experimental setup. The 200[Hz] sinusoid we synthesized and memoried on a CD was amplified through an audio amplifier(Bose; 1701II) and output by a speaker(Bose; 101MM) fixed right above on the sensor by 30[cm]. In the setup, the directivity of the speaker gives little influence to experimental results since it is considered that the directivity is small on the low frequency (the sound source signal is sinusoids of 200Hz as mentioned) and the sensor is always located in the front of the speaker. The sensor and measurement system are mounted on two rotational stages as shown in Fig.10 so that we can adjust the direction of the sound source by inclining and rotating them relative to the sound source.

The vibration of the diaphragm was measured by a laser displacement sensor (Keyence; LC-2430), digitized by an A/D board (Interface; PCI-3163), and analyzed on a desktop PC. In this system, we can observe only one point on the diaphragm at once. So, by using the sound source signal, we synchronized vibration waveforms, $z_i(t)$ at four points $(i = A, B, C, D)$ shown in Fig.11 . Then, we obtained in-phase, x-axis reversed-phase, and y-axis reversed-phase components of the diaphragm vibration by $(z_A(t) + z_B(t) + z_C(t) + z_D(t))/4$,

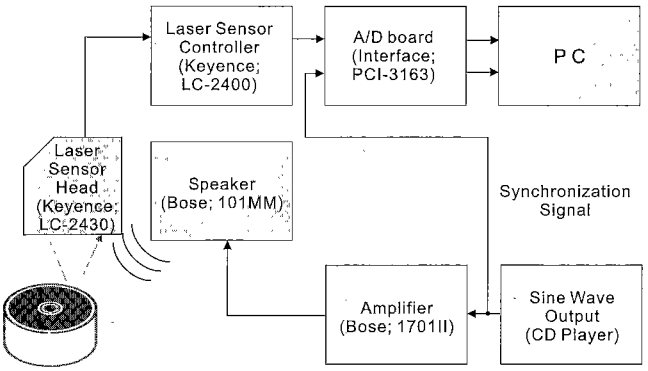

Fig. 9. A schematic diagram of the experimental setup.

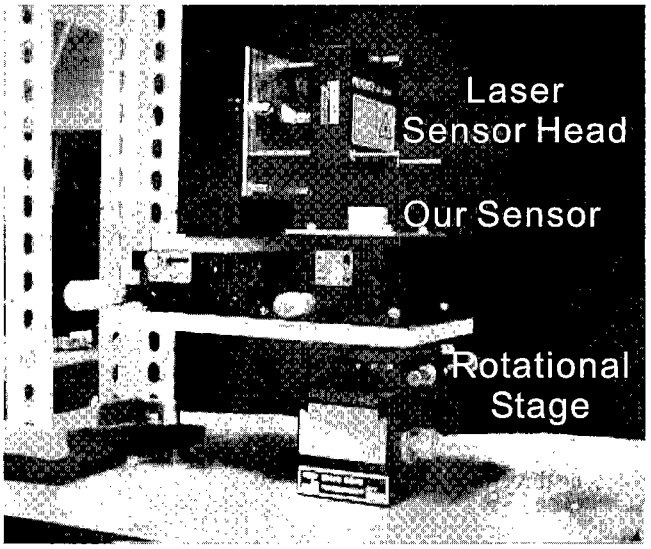

Fig. 10. A picture of the experimental setup.

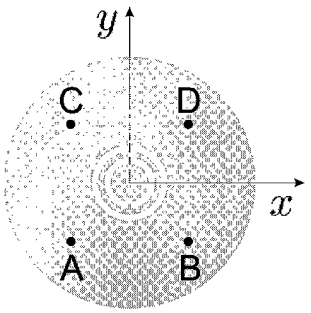

Fig. 11. Four measurement points on the diaphragm. The distance between the neighboring points is 10[mm].

$(-z_A(t) + z_B(t) - z_C(t) + z_D(t))/4$, and $(-z_A(t) - z_B(t) + z_C(t) + z_D(t))/4$, respectively. In order to investigate the vibration of the diaphragm in high S/N ratio, each signal is obtained by 500 times synchronized accumulation for noise reduction.†

4.3 Results Fig.12 shows the vibration wave-

† In practical situation, we don't apply synchronous accumulation because an input signal is unknown. But, the short-time correlation in the localization algorithm works as a noise reduction process. The introduction of the efficient transduction mechanism to the sensor will improve the S/N ratio of the sensor signal and reduce the necessary integral interval.

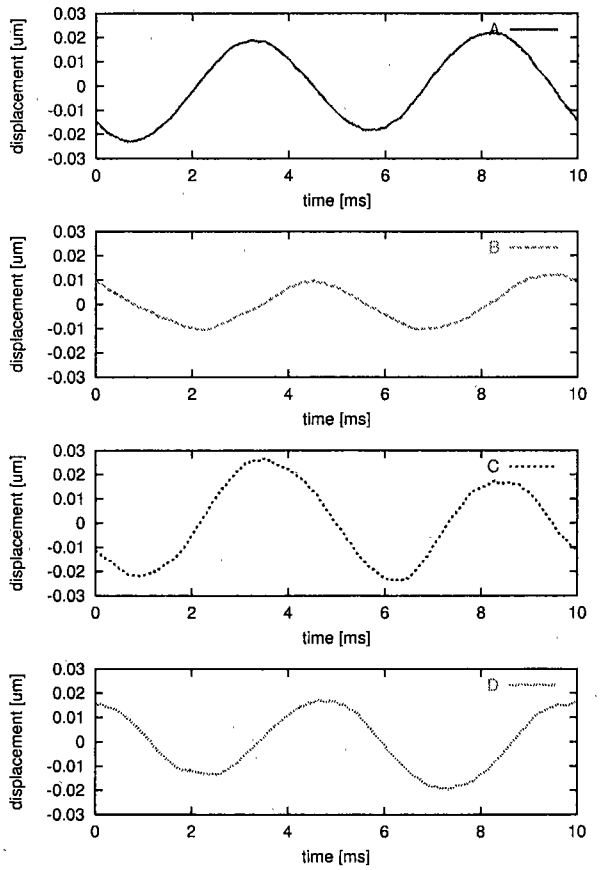

Fig. 12. The vibration waveforms on four measurement points, A, B, C, D, from top to bottom. The direction of sound source is $(\phi,\ \theta) = (\pi/12,\ 0)$.

forms on four measurement points when the direction of sound source is $(\phi,\ \theta) = (\pi/12,\ 0)$. These graphs clearly indicate that A, C and B, D vibrates in different phase and the gimbal diaphragm detects a very small acoustic gradient. The vibration displacement is about $0.02[\mu\mathrm{m}]$.

Fig.13 shows in-phase, x-axis reversed-phase, and y-axis reversed-phase components of the vibration in two cases: $(\phi,\ \theta) = (\pi/12,\ 0), (\pi/12,\ -\pi/2)$. We can confirm that the reversed-phase vibrations are depend on the sound source direction, while the in-phase vibration is independent of it because the former is driven by the sound gradient and the latter is driven by the sound pressure. The fact is also in coincidence with our theory that the phase difference between the in-phase and the reversed-phase signals is $\pi/2$.

Fig.14 shows an experimental result of the sound source localization. The true sound source directions (open circles) and localized directions (closed circles) are represented by S_x and S_y defined by eq.(14), eq.(15). A large circle indicates $\phi = \pi/12$. In this experiment, we determined the constant, C in eq.(16) experimentally. Since it can be regarded as fitting about ϕ, the errors of ϕ are less than those of θ. Fig.15 shows another result of the sound source localization when the sound source signal is 400[Hz] sinusoid. In both cases, the sound source is localized in almost right directions.

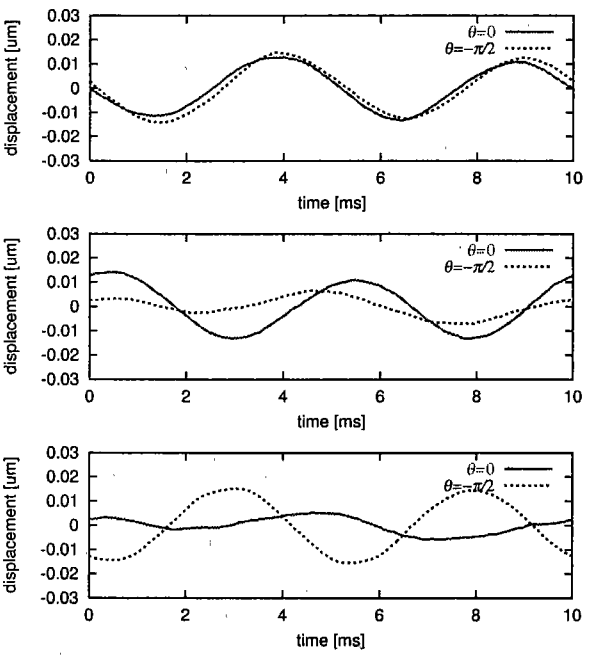

Fig. 13. Three components of the vibration: the in-phase (top), the x-axis reversed-phase (center), and the y-axis reversed-phase components (bottom). The directions of the sound source are $(\phi,\ \theta) = (\pi/12,\ 0), (\pi/12,\ -\pi/2)$.

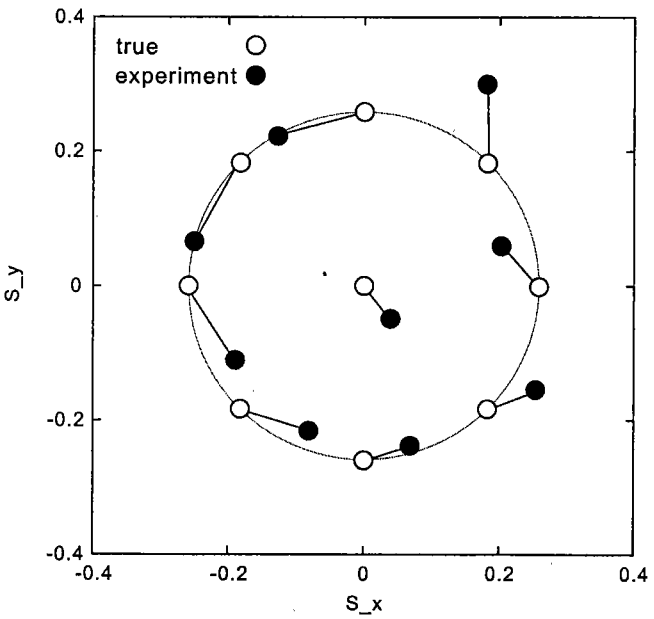

Fig. 14. The sound source localization result when the sound source signal is 200[Hz] sinusoid. The horizontal and the vertical axis represent $\sin\phi\cos\theta$ and $\sin\phi\sin\theta$, respectively.

5. Conclusion

In this paper, with mimicking an excellent mechanism of the parasitoid fly's ear, we proposed a gimbal diaphragm, which realizes a simple and optimal transduction mechanism for a very small pressure gradient caused by the sound field. As a first step to realize a micro sound source localization sensor, we fabricated

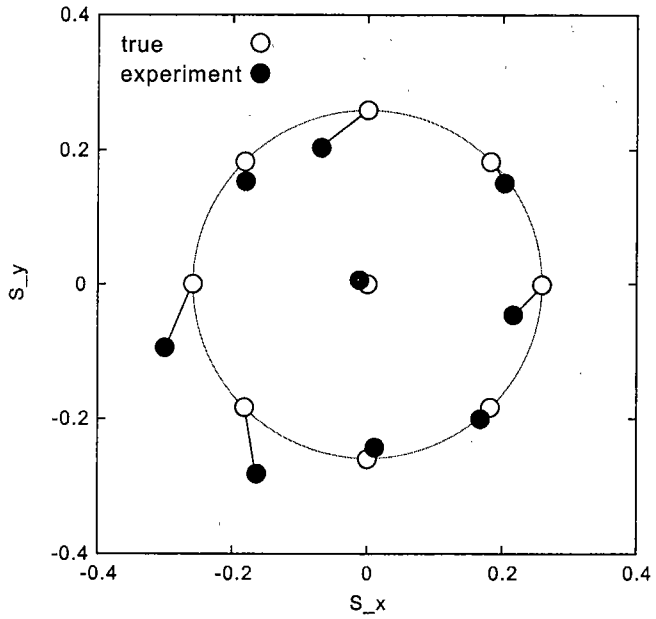

Fig. 15. The sound source localization result when the sound source signal is 400[Hz] sinusoid. The horizontal and the vertical axis represent $\sin\phi\cos\theta$ and $\sin\phi\sin\theta$, respectively.

a model diaphragm by thin metal plate and confirmed that 1) it detects a very small sound gradient, 2) it localizes the direction of the sound source as the theory, by experiments.

The subjects of succeeding works will be the establishment of strict design rules of the diaphragm and the introduction of the efficient transduction mechanism from mechanical vibrations to electric signals. We are considering 1) piezoresistive transduction: placing piezoresisters on the ring and the beams of the gimbal, where the deformation of the diaphragm is concentrated, and detecting the vibration by strains there, 2) capacitive transduction: forming four condensers with the diaphragm and back-electrodes separated into 2×2 cells and detecting the vibration capacitively. In both cases, good agreement with the Si micromachining process is the most important concern for us.

Acknowledgment

This work was partially supported by a research grant of the Sound Technology Promotion Foundation.

(Manuscript received June 24, 2002, revised November 7, 2002)

References

(1) J. Blauert: "Spatial Hearing", MIT Press, Cambridge, MA, (1983)

(2) E. I. Knudsen: "The Hearing of the Barn Owl", *Sci. Amer.*, Vol. 245, No. 6, pp.83–91 Dec. (1981)

(3) D. Robert, J. Armoroso, and R. R. Hoy: "The Evolutionary Convergence of Hearing in a Parasitoid Fly and Its Cricket Host", *Science*, Vol. 258, pp. 1135–1137 Nov. (1992)

(4) D. Robert, M. P. Read, and R. R. Hoy: "The tympanal hearing organ of the parasitoid fly *Ormia ochracea* (Diptera, Tachinidae, Ormiini)", *Cell Tissue Res.*, Vol. 275, pp. 63–78 Nov. (1994)

(5) R. N. Miles, D. Robert, and R. R. Hoy: "Mechanically coupled ears for directional hearing in the parasitoid fly *Ormia ochracea*", *J. Acoust. Soc. Am*, Vol. 98, No. 6, pp. 3059–3070 Dec. (1995)

(6) A. C. Mason, M. L. Oshinsky, and R. R. Hoy: "Hyperacute directional hearing in a microscale auditory system", *Nature*, Vol. 410, pp. 686–690, 5 Apr. (2001)

(7) N. Ono, T. Hirata, and S. Ando: "A Study on Sound Source Localization Sensor with Mimicking Ormia Ochracea's Ears", *Technical Digest of the 18th Sensor Symposium*, pp. 351–354 Kawasaki, May (2001)

(8) "http://www.me.binghamton.edu/NIH%20visit/sld002.htm"

(9) S. Ando, H. Shinoda, K. Ogawa, and S. Mitsuyama: "A Three-Dimensional Sound Localization Sensor System Based on the Spatio-Temporal Gradient Method", *Trans. Soc. Instrument and Control Engineers (SICE)*, Vol.29, No.5, pp.520-528 (1993)

Nobutaka Ono (Member) received B.E. M.S. and Ph.D degrees in mathematical engineering and information physics from the University of Tokyo, in 1996, 1998, 2001, respectively. He joined the Graduate School of Information Sience and Technology, University of Tokyo in 2001 as a Research Associate. His research interest is in the area of auditory modeling and acoustic sensing. He is a member of IEEJ, SICE, ASJ and ASA.

Akihito Saito (Non-member) received B.E. degree in mathematical engineering and information physics from University of Tokyo, in 2002. He is currently a master course student at the Graduate School of Engineering, University of Tokyo. His resarech interest is in the area of acoustic sensing.

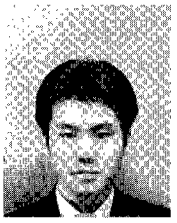

Shigeru Ando (Member) received the B.E., M.S., and Ph.D degrees in mathematical engineering and information physics from the University of Tokyo in 1974, 1976, and 1979, respectively. He joined the Faculty of Engineering of the University of Tokyo in 1979, served as Associate professor from 1987, and is currently Professor at the Department of Mathematical Engineering and Information Physics, Graduate School of Engineering of the University of Tokyo.

He works on research and education on sensors, image processing, signal processing, optical and acoustic sensing, measurement, and electric circuits. His interests are on intelligent and smart sensing structure and artificial implementation of sensing and perception of human being (see "http://www.alab.t.u-tokyo.ac.jp/~ando" for more detail). In 1978, 1987, 1993, and 1998, he received the annual paper awards from the Society of Instrument and Control Engineers (SICE).

He is a member of IEEE, the Optical Society of America, the Acoustical Society of America, the steering committee of Conference of Solid-State Sensors and Actuators (Transducers), and many Japanese academic societies such as the Institute of Electrical Engineers of Japan (IEEJ), the Acoustical Society of Japan, the Optical Society of Japan, Information Processing Society of Japan, and the Society of Instrument and Control Engineers (SICE).